RSC Advances

ROYAL SOCIETY OF CHEMISTRY

www.rsc.org/advances

Four novel metal-quinolone complexes tightly binded to calf-thymus DNA and exhibited good binding propensity to albumin protein.

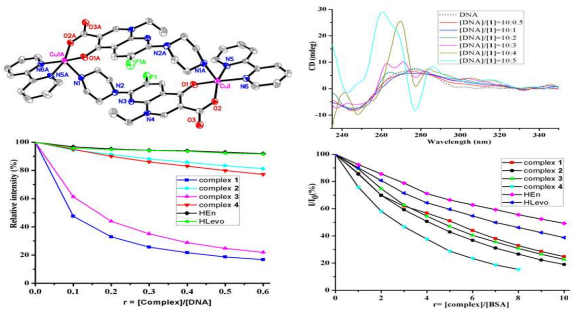

Cu(II) and Co(II) ternary complexes of quinolone antimicrobial drug enoxacin and levofloxacin: Structure and biological evaluation

Wan-Yun Huang[a,b,d,1], Ji Li[c,1], Shi-Lin Kong[d], Zhong-Chang Wang[a], Hai-Liang Zhu[a,*]

[a]*State Key Laboratory of Pharmaceutical Biotechnology, Nanjing University, Nanjing 210093, China.*

[b]*Department of Pharmacology, Guilin Medical University, Guilin 541004, China.*

[c]*School of Life Sciences, Shandong University of Technology, Zibo 255049, China.*

[d]*Key Laboratory for the Chemistry and Molecular Engineering of Medicinal Resources (Guangxi Normal University), Ministry of Education of China, Guilin 541004, China..*

[1] These authors contributed equally to this work.

*Corresponding author. Tel. & fax: +86-25-83592672; e-mail: zhuhl@nju.edu.cn (H.L. Zhu).

ABSTRACT

Four complexes of the quinolone antibacterial agent enoxacin (HEn) and levofloxacin (HLevo) with Cu^{2+} and Co^{2+} have been synthesized and characterized by physicochemical and spectroscopic techniques. Complex **1** is a novel dinuclear structure, in which enoxacin exhibits a tridentate binding mode bound to two Cu(II) ions through the pyridone oxygen, the carboxylate oxygen and the piperazine nitrogen atom, so far as we know such mode and structure had never been presented before in metal-quinolone complexes. In mononuclear complexes **2**-**4**, enoxacin and levofloxacin act as a bidentate ligand bound to the metal through the ketone oxygen and a carboxylate oxygen atom. The antimicrobial activity of the complexes **1**-**4** against four bacterial species were tested and the results indicated that they exhibit enhanced or similar activity to the free ligands. Studies on the interaction of **1**-**4** with calf-thymus (CT) DNA through UV and circular dichroism (CD) spectroscopies indicated that they bind to CT DNA probably by the intercalative binding mode. Fluorescence competitive studies with ethidium bromide (EB) revealed that the complexes could compete with EB and displace them to bind to DNA using the intercalative binding site. In addition, the complexes **1**-**4** exhibited good binding propensity to human and bovine serum albumin proteins with relatively high binding constants.

Keywords: Enoxacin; Levofloxacin; Quinolones; Cu(II) complex; Co(II) complex; Biological evaluation

Introduction

Quinolones are a large family of synthetic antibacterial agents with a 4-oxo-1,4-dihydroquinoline skeleton, which have been developed for clinical use in human medicine for the treatment of a variety of infections by targets to the bacterial type II DNA topoisomerases.[1-4] Despite their widespread application, so far the detailed mechanism of the biological action of them is still not fully understood. Some evidence suggests that these drugs interact directly with DNA, blocking the activity of DNA-gyrase repair enzymes. Other discoveries of topoisomerase-DNA-quinolone complex suggest that the metal ions play an important role in the action mechanism of these drugs.[2] The chelation between the metal ion and the carbonyl and carboxyl groups of the quinolones as well as the binding of the resulting complex to DNA may be the essential prerequisites for their antibacterial activity.[5-7] So, in recent years, numerous studies about the interaction between series of quinolones and metal cations have been reported and reviewed in the literature.[2,8–19] The previous results showed that the modes of metal coordination with quinolone ligands are influenced by number of factors, such as method of crystallization, the pH value of the reaction solution, the counter ion and ancillary ligands. Especially, the mixed-ligand metal complexes of quinolones are found to exhibit enhanced biological activities.[20,21] In particular, the study of quinolones–copper–phen complexes has attracted much attention since they seem to exhibit high affinity to DNA binding as well as nuclease activity to plasmid, genomic and internucleosomal DNA.[22,23]

Enoxacin (HEn) (Scheme 1a) is one of the third-generation members of quinolone antibiotics fluorinated in position C-6 and bearing a piperazinyl moiety in position C-7. It

kills bacteria through inhibiting cell DNA-gyrase and prohibiting DNA replication and transcription.[24-25] In literature, the crystal structures of Cu(II), Ni(II), Co(II), Zn(II), Cd(II), Mn(II), Ag(I) binary enoxacin complexes have been reported [26-30], and the results suggested that metal ion coordination might be involved in the antibacterial activity of drug molecules and improve the drugs activity. To the best of our knowledge, no crystal structures of ternary metal complexes of enoxacin have been published yet. Levofloxacin (HLevo)(Scheme 1b), is the *L*-isomer of the racemate ofloxacin, considered as a third-generation quinolone antimicrobial agent with a very successful clinical track record and commonly used for the treatment of respiratory, genitourinary and gastrointestinal tracts as well as skin and soft tissue infections.[31-33] A thorough survey of the literature has revealed that only several single crystal structures of binary levofloxacin complexes have been characterized, including a Mg(II),[34] three Cu(II), [6,35,36] two Zn(II),[37,38] and two Ru(II) ones,[39,40] and at present only one crystal structure Cu(levo)(phen)(H_2O)(NO_3)·2H_2O about the ternary complex of levofloxacin has been reported [41].

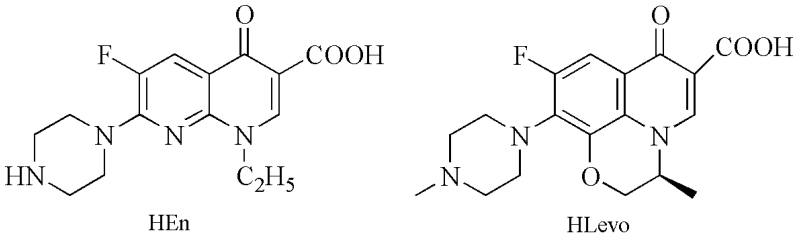

Scheme 1. (a) Enoxacin (HEn) and (b) Levofloxacin (HLevo)

Copper is a physiologically relevant metal that plays a significant role in many biological processes and exhibits considerable biochemical action.[42] Current interest in copper

complexes origins in its role in proteins as well as its potential synergetic activity with antimicrobial, antiviral or even antitumor drugs.[43,44] The biological role of cobalt is attributed not only its presence in the active center of vitamin B_{12} which regulates indirectly the synthesis of DNA and several cobalt-dependent proteins but also to biological activity exhibited by its complexes.[45,46] Due to the important biological role of copper and cobalt and the existence of a potential synergetic activity when administrated with drugs, we pay our attention to investigate the interaction of Cu(II) or Co(II) complexation with fluoroquinolones.

In this paper, we report the syntheses, characterizations and crystal structure of four ternary Cu(II) and Co(II) complexes with enoxacin or levofloxacin in the presence of the N-donor heterocyclic ligands 2,2′-bipyridine (bipy) or 1,10-phenanthroline (phen), namely $Cu_2(En)_2(bipy)_2 \cdot 2(ClO_4) \cdot 3(H_2O)$ (**1**), $Co(En)(HEn)(bipy) \cdot (ClO_4) \cdot 4(H_2O)$ (**2**), $Cu(Lev)(bipy)(H_2O) \cdot (ClO_4) \cdot 2(H_2O)$ (**3**), $Co(HLev)_2(phen) \cdot 2(ClO_4) \cdot 8(H_2O)$ (**4**). In order to investigate the possibility of existence of any potential biological activity of complexes **1**−**4** the study has been focused on (i) the interaction of the complexes with calf-thymus DNA (CT DNA) investigated by UV spectroscopy, Circular dichroic (CD) spectra; (ii) the ability to displace ethidium bromide (EB) from the classical DNA-intercalator EB performed by fluorescence spectroscopy, (iii) the affinity of the complexes to bovine (BSA) and human serum albumin (HSA) binding properties investigated by fluorescence spectroscopy, and (iv) the antibacterial activity of the complexes by the minimum inhibitory concentration (MIC) against four microorganisms.

Experimental section

Materials

All reagents were commercially available and used as received without further purification unless noted specifically. Tris-HCl-NaCl (TBS) buffer solution (5 mM Tris, 50 mM NaCl, pH adjusted to 7.30 by titration with hydrochloric acid using a Sartorius PB-10 pH meter, Tris = tri(hydroxymethyl)aminomethane) was prepared using double distilled water. Bovine serum albumin protein (BSA) and human serum albumin protein (HSA) were purchased from Sigma. Calf thymus DNA (CT-DNA) was purchased from Sino-American Biotech Co., Ltd. (Beijing). DNA stock solution was prepared by dilution of CT DNA to TBS buffer followed by exhaustive stirring for three days, and kept at 4 °C for no longer than a week. The stock solution of CT DNA gave a ratio of UV absorbance at 260 nm and 280 nm (A_{260}/A_{280}) of 1.83, indicating that the DNA was effectively free of protein contamination.[47] The DNA concentration pernucleotide was determined by the UV absorbance at 260 nm after 1:20 dilution employing a molar absorption coefficient (6600 M^{-1} cm^{-1}).[48]

Caution! Perchlorate complexes are potentially explosive. The experiments were carried out in an isolated room and the operator must be protected with blast shield and other necessary equipments. The perchlorate complexes should be prepared only in small amount and handled with extreme care.

Physical measurements

Infrared spectra were recorded as KBr pellets using a Perkin-Elmer FT-IR Spectrometer. Elemental analyses (C, H and N) were performed on a PerkinElmer Series II CHNS/O 2400

elemental analyzer. ESI-MS spectra were performed on Thermofisher Scientific Exactive LC-MS Spectrometer. UV−vis absorption was performed on a Varian Cary100 UV−visible spectrophotometer. Fluorescence spectra were recorded in solution on a Shimadzu RF-5301/PC spectrofluorophotometer. The Circular dichroic spectra of DNA in the region between 200 and 400 nm were obtained by using a JASCO J-810 automatic recording spectropolarimeter operating at 25 °C.

Antimicrobial activity studies

Two different cultivation media were used for antimicrobial activity test: (1) Luria-Bertani broth (LB) medium, containing 1% tryptone, 0.5% NaCl and 0.5% yeast extract and (2) minimal medium salts broth (MMS), containing 1.5% glucose, 0.5% NH_4Cl, 0.5% K_2HPO_4, 0.1% NaCl, 0.01% $MgSO_4 \cdot 7H_2O$ and 0.1% yeast extract. The pH of the media was adjusted to 7.0.

The antibacterial efficiency of the compounds (ligands, metal salts and complexes **1**-**4**) were estimated by their ability to inhibit the growth of microorganisms in the cultivation medium. The tests were performed according to minimum inhibitory concentration (MIC) in μg mL^{-1} with four bacteria species: Escherichia coli (*E. coli*), Pseudomonas aeruginosa (*P. aeruginosa*), Bacillus subtilis (*B. subtilis*) and Staphylococcus aureus (*S. aureus*). Bacterial growth was performed in LB, while the screening for antibacterial activity was performed by the MIC method,[41] using the method of progressive double dilution in MMS contained the concentrations of 100, 50, 20, 10, 5, 2.5, 1.25 μg mL^{-1} of the complexes in DMSO were tested and the MICs were determined. Two milliliters of MMS were inoculated with 20 μL of a preculture of each bacterial strain, which was grown in LB overnight at the optimal growth

temperature of each species to assure the sufficient bacterial growth. In a similar second culture, 20 μL of the bacteria as well as the tested compound at the desired concentration were added. A third sample was supplemented with the same concentration of the compounds tested and was used as cultures of reference to check the effect of each compound on MMS. All samples were measured in duplicate. The stock solutions of the compounds (10 mg mL^{-1}) were prepared by previously dissolving in DMSO. Then twofold serial dilutions were carried out in MMS to introduce the compounds at a final concentration ranging from 10 to 0.125 μg mL^{-1} to the cultures. The bacterial growth was monitored by measuring the turbidity of the culture after 24 h in order to check if bacteria grow at the concentration of compound tested. The lowest concentration that inhibited bacterial growth was determined as the MIC value. All the equipment and culture media were sterile.

Synthesis of the complexes 1-4

$Cu_2(En)_2(bipy)_2 \cdot 2(ClO_4) \cdot 3(H_2O)$ (1)

A methanolic solution (15 mL) of enoxacin (0.1280 g, 0.4 mmol), bipy (0.0312 g, 0.2 mmol) and KOH (0.0224 g, 0.4 mmol), was added dropwise to a methanolic solution (5 mL) of $Cu(ClO_4)_2 \cdot 6H_2O$ (0.0741 g, 0.2 mmol) and the reaction mixture was refluxed for 2 h. The resultant solution was filtered and left for slow evaporation. Green crystals of **1**, suitable for X-ray structure determination were collected after a couple of days. Yield: 77.8 mg, 60%. Anal. Calcd. for $C_{50}H_{54}N_{12}O_{17}F_2Cl_2Cu_2$ (Mr = 1331.04): C 45.12, H 4.09, N 12.63; found C 44.89, H 3.95, N 12.41. IR (KBr pellet, ν_{max}/cm^{-1}): 3437 (w), 1640 (vs), 1616 (m), 1524 (s), 1481 (m), 1444 (m), 1261 (s), 1098 (s), 772 (m), 626 (m). ESI-MS: *m/z* 1177.3 for $[Cu_2(En)_2(bipy)_2]^{2+}$.

Co(En)(HEn)(bipy)·(ClO_4) ·4(H_2O) (2)

Complex **2** was prepared in a similar way to that of **1** with the use of the corresponding $Co(ClO_4)_2·6H_2O$ (0.0733 g, 0.2 mmol). Orange crystals of **2** were deposited after a few days. Yield: 108 mg, 53%. Anal. Calcd. for $C_{42}H_{51}N_8O_{14}F_2ClCo$ (Mr = 1024.29): C 49.25, H 5.02, N 10.94; found C 50.84, H 4.86, N 11.27. IR (KBr pellet, ν_{max}/cm^{-1}): 3433 (w), 1605 (s), 1470 (m), 1441 (m), 1316 (s), 1093 (s), 765 (m), 617 (m). ESI-MS: *m/z* 534.2 for $[Co(En)(bipy)]^+$.

Cu(Lev)(bipy)(H_2O)·(ClO_4) ·2(H_2O) (3)

Complex **3** was prepared in a similar way to that of **1** using levofloxacin (0.1445 g, 0.4 mmol) instead of enoxacin. After a few days green crystals of **1** suitable for X-ray structure determination were collected. Yield: 74.8 mg, 51%. Anal. Calcd. for $C_{28}H_{33}N_5O_{11}FClCu$ (Mr = 733.58): C 45.84, H 4.53, N 9.55; found C 45.71, H 4.09, N 9.49. IR (KBr pellet, ν_{max}/cm^{-1}): 3401 (w), 1630 (s), 1586 (m), 1518 (s), 1465 (m), 1277 (m), 1101 (s), 770 (m), 614 (m). ESI-MS: *m/z* 579.2 for $[Cu(Lev)(bipy)(H_2O)]^+$.

$Co(Lev)_2$(phen)·2(ClO_4)·8(H_2O) (4)

Complex **4** was prepared in a similar way to that of **1** with the use of the corresponding N,N-donor ligand phen (0.0396 g, 0.2 mmol), levofloxacin (0.1445 g, 0.4 mmol) and $Co(ClO_4)_2·6H_2O$ (0.0733 g, 0.2 mmol). After a few days red crystals of **5** suitable for X-ray structure determination were collected. Yield: 117 mg, 45%. Anal. Calcd. for $C_{48}H_{64}N_8O_{24}F_2Cl_2Co$ (Mr = 1304.91): C 44.18, H 4.94, N 8.59; found C 44.61, H 4.53, N 8.78. IR (KBr pellet, ν_{max}/cm^{-1}): 3424 (s), 1624 (s), 1580 (s), 1471 (m), 1393 (m), 1276 (s), 1093 (s), 981 (m), 626 (m). ESI-MS: *m/z* 1060.2 for $[Co(Lev)_2(phen)]^{2+}$.

X-ray crystal structure determination

Suitable single crystals of **1**–**4** were selected and mounted onto thin glass fibers. Measurements of **1** were taken at 273(2) K using a Bruker CCDArea Detector with graphite-monochromated Mo-K_α radiation (λ = 0.71073 Å). Measurements of **2-4** were taken at 296(2) K using a Agilent CrysAlisPro Detector in the same radiation. All the structures were solved by direct methods using the *SHELXS-97* program package and refined against F^2 by full-matrix least-squares methods with *SHELXL-97* [49,50] with anisotropic thermal parameters for all the non-hydrogen atoms. Hydrogen atoms attached to carbon were placed in geometrically idealized positions and refined by using a riding model. Hydrogen atoms attached to water oxygen atom O17 of **1**, O13 of **2** and all the water oxygen atoms of **4** were not located from difference Fourier maps or positioned in calculated positions, so they were not included in the refinement, but they were added to the molecular formula of the complex. Hydrogen atoms on other water oxygen atoms were located from difference Fourier maps and refined by using a riding model. A summary of crystallographic and structural refinement data for **1**–**4** is given in Table 1. Selected bond lengths and bond angles are listed in Table S1. Hydrogen bonds are listed in Table S2.

<<<Insert Table 1 here>>>

DNA binding studies

The synthesized complexes **1**–**4** and ligand were dissolved in DMSO to make 2.0 mM stock solutions for DNA binding studies. The final working solutions of the complexes for

DNA binding studies are diluted in the TBS and the containing DMSO is limited in 1%. In UV absorption spectrometry, the working solutions of the complexes are 10 μM. After each addition, the solution was allowed to incubate for 10 min before the absorption spectra were recorded. The binding constants (K_b) of the compounds with CT DNA have been determined using the UV spectra of the compound recorded for a constant concentration in the absence or presence of CT DNA for diverse compound/CT DNA mixing ratios (r).

In the CD absorption spectrometry, the working solution of the complexes were prepared by using 1×10^{-4} M DNA and titrating the complexes into the DNA solution stepwise in a ratio value of DNA/compound from 10:0.5 to 10:6. The working solution was incubated for 5 min after each addition and then its CD spectrum was recorded at 100 nm/min scan rate. The CD signals of the TBS were subtracted as the background.

A solution containing 10^{-4} M DNA and 10^{-5} M EB (DNA/EB = 10:1) were prepared for CT DNA–EB competitive binding studies. The intercalating effect of complexes **1**–**4** with the DNA–EB complex was studied by adding a certain amount of a solution of the compound step by step into the solution of the DNA–EB complex. The influence of the addition of each compound to the DNA–EB complex solution has been obtained by recording the variation of fluorescence emission spectra.

Albumin binding experiments

The protein binding study was performed by tryptophan fluorescence quenching experiments using bovine (BSA, 3 μM) or human serum albumin (HSA, 3 μM) in buffer (containing 15 mM trisodium citrate and 150 mM NaCl at pH 7.0). The quenching of the emission intensity of tryptophan residues of BSA at 343 nm or HSA at 351 nm was monitored

using complexes **1**–**4** as quenchers with increasing concentration.[51] Fluorescence spectra were recorded at an excitation wavelength of 295 nm in the range 300–500 nm. The fluorescence spectra of HEn, HLevo ligands and the complexes **1**–**4** were recorded under the same experimental conditions. The quantitative studies of the serum albumin fluorescence spectra were performed after their correction.

Results and discussion

Synthesis and spectroscopic study

The synthesis of the complexes was achieved via the reaction of the quinolone, deprotonated with KOH, in the presence of the corresponding N-donor ligand (bipy or phen) with metal perchlorate salts under the same reflux condition. The resultant complexes are soluble in DMSO and DMF.

In order to confirm the deprotonation and binding mode of the quinolones, IR spectroscopy may be a useful technique. In the IR spectra of complexes **1**-**4**, the observed absorption band at 3414 (br,m) cm^{-1} and 3433 (br, m) cm^{-1} attributed to the ν(O−H) stretching vibration of HEn and HLevo molecule, respectively, have disappeared upon binding to the metal ion which is indicative of deprotonation of the carboxylate group. The absorption bands at 1624 (br) cm^{-1} and 1270 (s) cm^{-1} attributed to the stretching vibrations $\nu(C{=}O)_{carboxylic}$ and $\nu(C{-}O)_{carboxylic}$, respectively, of the carboxylic group (−COOH) of enoxacin, have been replaced in the IR spectra of **1** and **2** by two strong characteristic bands in the range 1640-1605 cm^{-1} and 1261-1453 cm^{-1}, indicating the carboxylate group coordinated to the metal. Levofloxacin showed the characteristic absorptions band for the carboxylic and the

pyridinone stretch at 1718 cm^{-1} and 1620 cm^{-1}, respectively. In complex **3** and **4**, the carboxylic stretch disappears and is replaced by two strong and characteristic bands assigned as asymmetric (1586 cm^{-1}, 1580 cm^{-1}) and symmetric (1465 cm^{-1}, 1395 cm^{-1}) vibrations. The difference $\Delta\nu_{asym}(C=O) - \nu_{sym}(C=O)$ reaches a value of 121 cm^{-1} and 185 cm^{-1}, which indicates a monodentate coordination mode of the carboxylate group.[52] The $\nu(C=O)_{pyridinone}$ vibration is slightly shifted in the spectra of **3** and **4** towards 1630 cm^{-1} and 1624 cm^{-1} upon binding. The overall changes of **1-4** suggest that HEn/HLevo is coordinated to the metal via the the pyridine oxygen and a carboxylato oxygen, which are in agreement with the reported chelating binding mode of the quinolones.[53] The strong band at 1093-1101 cm^{-1} in **1-4** corresponds to a $\nu(ClO_4)^-$ vibration confirming the presence of a free ClO_4^- group.

Complexes **1-4** are soluble at 2×10^{-5} M concentration level in the TBS buffer solution at 25 ℃ containing 1% DMSO. The kinetic stability of **1-4** (Fig. S1) was evaluated by UV−vis absorption under this condition. Over the time course, the characteristic absorption of each complex all showed hypochromicity but no bathochromic shift. The hypochromicity can be attributed to the gradual formation of aggregates of the complexes in solution, which will decrease their effective concentration for UV−vis absorption.[54] The spectra indicates that the inner-sphere of complexes **1-4** keep their integrity in buffer.

Crystal structure description

Crystal structure of $Cu_2(En)_2(bipy)_2 \cdot 2(ClO_4) \cdot 3(H_2O)$ (1)

Complex **1** is a discrete dinuclear structure and crystallizes in the triclinic crystal system $P\bar{1}$ space group. To our best knowledge, dinuclear structure is scarce in number of reported structurally characterized metal–quinolone complexes and such dinuclear structure bridging

through oxygen and nitrogen atoms of quinolone ligands has never been presented before. The asymmetric unit of **1** is composed of two crystallographically independent Cu(II) ions, two deprotonated En ligand, two bipy mixed ligands, two ClO_4^- counter ions and three guest water molecules. Cu1 and Cu2 exist in two similar crystallographically independent dinuclear molecules which present differences in bond distances and angles (Table S1). As shown in Fig. 1, the En ligand exhibits tridentate binding mode bound to two Cu(II) ions through the pyridone oxygen, the carboxylate oxygen and the piperazine nitrogen atom, forming a square motif in which the corner is occupied by each Cu(II) ion. Both Cu(II) ions (Cu1 and Cu2) exhibit similar coordination environment, so the Cu1 is discussed in detail as a representative. The Cu1 is five-coordinated in a slightly distorted square-pyramidal geometry with one carbonyl oxygen atom (O1), one carboxylate oxygen atom (O2) from one En ligand and two nitrogen atoms (N5 and N6) from the bipy in the equatorial plane, and one nitrogen atom (N1A) from the other En ligand occupied the axial position. The geometrical parameter $\tau = (\alpha-\beta)/60^{\circ}$, where β and α are the two largest angles in the coordination sphere of the metal; $\tau = 0$ for a perfect square pyramid and $\tau = 1$ for a perfect trigonal bipyramid) τ is 0.089, indicating little distortion from the regular square-based pyramidal geometry.[55] The Cu1 deviates 0.2566(5) Å from the basal plane in direction of the N1A atom. The trans atom system of the basal plane gives angles of O(1)–Cu(1)–N(6) = 166.1(3)º and O(2)–Cu(1)–N(5) = 160.7 (3)º. The distances of the piperazine nitrogen atom and Cu (Cu1-N1 = 2.278 Å, Cu2-N7 = 2.291 Å) are the longest distances in the coordination sphere of Cu. The N(5)-Cu(1)-N(6) and N(11)-Cu(2)-N(12) angles are 81.1(3)° and 80.7(3) ° respectively, which is similar to reported values of other chelating bipyridine complexes.[53] In the dinuclear structure of **1**, Cu1 and

Cu1A is separated by En ligand with the distances of 10.84(3) Å.

The crystal structure is further stabilized by π–π stacking between the aromatic planes of the En ligands and bipyridine with the centroid···centroid separation of 3.77 Å (Fig. S2) and by the hydrogen bonds between guest water molecules and the uncoordinated carboxylic oxygen atoms (Table S2).

<<<Insert Figure 1 here>>>

Crystal structure of Co(En)(HEn)(bipy)·(ClO_4)·4(H_2O) (2)

Complex **2** is a mononuclear cationic complex of cobalt (Fig. 2) where the cationic unit of $Co(En)(HEn)(bipy)^+$ is neutralized by an anion ClO_4^-. The Co(II) ion is six-coordinated in a distorted octahedral geometry by two O_{keto} atoms (O1, O4) and two $O_{carboxylate}$ atom (O2, O5) from two different enoxacin ligands and two nitrogen atoms (N7, N8) from one bipy ligand. In **2**, enoxacin is present in both its neutral and its anionic forms. In the neutral zwitterionic form (HEn), the piperazinyl ring is protonated on the external nitrogen atom (N3). The arrangement of two enoxacin ligands is such that two carboxylato oxygen atoms, O2 and O5 (O2-Co1-O5 = 175.81(10)º), are in *trans* and two pyridine oxygen atoms, O1 and O4, (O1-Co1-O4 = 89.40(10)º) are in *cis* arrangement. The planes containing the ethyl group carbon atoms are almost perpendicular to the enoxacin ring systems; the torsion angles are: C(9A)–N(1A)–C(10A)–C(11A) 89.8(10)º. The Co–O and Co–N bond distances are in the range of 2.046–2.106 Å. The distances and angles in the quinolone ring systems, as well as those of the piperazine rings, are similar to those found in reported structures of free enoxacin

compounds.[26-28] The piperazinyl rings are non-coplanar with the quinolone rings and adopt a normal chair conformation.[56]

Hydrogen bonds among guest water molecules, carboxylato oxygen atom, nitrogen atom of piperazine and oxygen atom of ClO_4^- (Table S2) are observed, which resulted in the formation of complicated 3D supramolecular framework.

<<<Insert Figure 2 here>>>

Crystal structure of Cu(Lev)(bipy)(H_2O)·(ClO_4)·2(H_2O) (3)

The crystal structure of **3** (Fig. 3) consists of a cationic mononuclear Cu(Lev)(bipy)$(H_2O)^+$, accompanied by a uncoordinated ClO_4^- anion and two guest water molecules. The copper ion is five-coordinate lying in a slightly distorted square–pyramidal geometry. Two oxygen atoms (O1 and O2) of levo ligand and two nitrogen atoms (N4 and N5) of the bipy ligand occupy the four positions in the basal plane, while an oxygen atom (O9) from one water molecule is in the apical position. The trigonality index τ = (170.47-168.065)/60º = 0.04. The Cu1 deviates 0.1509 Å from the basal plane toward the apex O9 atom. The trans atom system of the basal plane gives angles of O1–Cu1–N4 = 170.49(11)º and O2–Cu1–N5 = 168.07(12)º. The distances between O9 atom of coordinated water and Cu1 (Cu1-O9 = 2.280(3) Å) are the longest distances in the coordination sphere of Cu. The ligand behaves as a bidentate ligand in deprotonated mode and is coordinated to the copper ion via the pyridone oxygen (O1) and a carboxylato oxygen (O2). The Cu1-O2 bond distance (1.912 Å) is slightly shorter than that of Cu1-O1 (1.937 Å). The arrangement of the

atoms around the Cu(II) ion in **3** is similar to that observed in the reported Cu(II) complex such as Cu(enrofloxacinato)(bipy)(H_2O)Cl [57] and Cu(phenoxyalkanoato)$_2$(bipy)(H_2O) [58] with coordinated O_{water} occupying the apical position. The 3-methyl-piperazinyl rings adopt a normal chair conformation, with similar torsion angles: N(2)–C(16)–C(17)–N(3) 56.8(4)º, N(2)–C(14)–C(15)–N(3) 57.9(4)º .

Hydrogen bonds among guest water molecules, carboxylato oxygen atom and oxygen atom of ClO_4^- and π–π stacking between the aromatic planes of the Levo ligand and bipy with the centroid···centroid separation of 3.56 Å resulted in the formation of 2D supramolecular framework (Fig. S3).

<<<Insert Figure 3 here>>>

Crystal structure of Co(HLevo)$_2$(phen)·2(ClO_4) ·8(H_2O) (4)

Complex **4** is a dicationic mononuclear complex Co(HLevo)$_2$(phen)$^{2+}$. Here, the +2 charge is neutralized by two ClO_4^- anions. In **4**, the Co(II) ion is six-coordinated showing a distorted octahedral environment with the coordination sphere filled with two nitrogen atoms (N4, N4A) from the phen ligand, two pyridone oxygen (O3, O3A) and two carboxylate oxygen (O2, O2A) from two different HLevo ligands (Fig. 4). The arrangement of two HLevo ligands is such that two carboxylato oxygen atoms, O2 and O2A, O(2)-Co1-O(2A) = 170.4º, are in *trans* and two pyridine oxygen atoms, O3 and O3A, O(3)-Co1-O(3A) = 96.5º are in *cis* arrangement. A similar arrangement of the pyridone and the carboxylato oxygen atoms around metal center has also been found in the crystal structures of Zn(sparfloxacinato)$_2$(phen),[59]

Zn(enrofloxacinato)$_2$(phen).[38] The N(4)-Co(1)-N(4A) angle observed is 78.7 (3)° and is similar to reported values of other chelating phen complexes.[21] The 3-methyl-piperazinyl rings adopt a normal chair conformation with torsion angles: N(2)–C(15)–C(167)–N(3) 61.36(4)°, N(2)–C(17)–C(18)–N(3) 57.186(1)°.

<<<Insert Figure 4 here>>>

Antibacterial activity

The efficiencies of the quinolone ligand, the co-ligand, the metal salts and the complexes **1**-**4** have been tested against two Gram(+), Bacillus subtilis (*B. subtilis*), Staphylococcus aureus (*S. aureus*) and two Gram(–), Escherichia coli (*E. coli*) and Pseudomonas aeruginosa (*P. aeruginosa*). The results of their antibacterial study are presented in Table 2.

<<<Insert Table 2 here>>>

HEn, HLevo, phen and the complexes **1**-**4** present inhibitory action against four microorganisms tested. Complex **1** exhibits higher activity to that of HEn against *B. subtilis* (MIC = 1.086 $\mu g \cdot mL^{-1}$) and *P. aeruginosa* (MIC = 1.685 $\mu g \cdot mL^{-1}$) and lower activity against *S. aureus* and *E. coli*. For Complex **2**, higher activity to that of HEn against *B. subtilis*, *S. aureus* and *P. aeruginosa* and lower activity against *E. coli* were presented. While the antimicrobial activity of complex **3** to that of free HLevo against *E. coli* has been improved, moreover providing the best inhibition against E. coli (MIC = 0.351 $\mu g \cdot mL^{-1}$) in the

synthesized four complexes by us. For complex **4**, only the activity to that of HLevo against *B. subtilis* has been improved, which exhibits the best inhibition among complexes **1**–**4** against B. subtilis (MIC = 0.066 $\mu g \cdot mL^{-1}$). The metal salts and bipyridine do not exhibit significant antimicrobial activity (MIC > 100 $\mu g \cdot mL^{-1}$) at the concentration range used to assay the activity of complexes **1**–**4** in this work.

As can be seen from the results, the antimicrobial inhibition (MIC = 0.066~4.087 $\mu g \cdot mL^{-1}$) of complexes **1**–**4** is inspiring although no clear trend can be ascertained whether the chelate effect or the nature of the N-donor ligands or other factors affect the final efficiency of each complex. In further studies, we will investigate their permeability, liposolubility, toxicity and the mechanism of antibiotic resistance.

Interaction with CT DNA

Investigations of the interaction of quinolones and their complexes with DNA is considerable important because their activity as antibacterial drugs is mainly focused on the inhibition of DNA replication by targeting essential type II bacterial topoisomerases. For quinolones and their metal complexes, DNA mainly provides three distinctive binding sites: groove binding, electrostatic binding to phosphate groups and intercalation.[2]

Study of the interaction with UV spectroscopy

The changes (hypochromism/hyperchromism and/or red shift/blue shift) observed in the UV spectra through titration may provide evidence of the existing interaction mode of quinolones and their metal complexes.

The UV spectra of a 1×10^{-5} M solution of the HEn/HLevo ligands or complexes **1**–**4** have been recorded during the titration upon gradually addition of CT DNA in diverse DNA/compound mixing ratios. In the UV spectrum of **1** (Fig. 5A), the band centered at 271

nm exhibits a hypochromism of 10% upon addition of increasing amounts of CT DNA, indicative of tight binding possibly by intercalation. The behavior of complexes **2**, **3** and HEn, HLevo upon addition of CT DNA is quite similar (Fig. S4). For **4**, the intensity of the bands centred at 272 nm and 287 nm (Fig. 5B) decreased in the presence of addition of CT DNA, also exhibiting a hypochromism. The observed hypochromism of the four complexes is due to stacking interaction between the aromatic chromophore (either from HEn/HLevo and/or the N-donor ligands) of the complexes and DNA base pairs consistent with the intercalative binding mode.[15, 60]

<<<Insert Figure 5 here>>>

The binding constant (K_b) of the compounds with CT DNA can be calculated by the ratio of slope to the intercept in plots DNA/(ε_a-ε_f) versus DNA (inset in Fig. 5) according to the equation Eq. (S1).[61] The calculated K_b values (Table 3) for the HEn, HLevo ligands and complexes **1**–**4** suggest a relatively moderate (for HEn, HLevo, **1**, **3** and **4**) to strong binding (for **2**) to CT DNA. Complex **2** exhibits the highest K_b value (=2.43(±0.36)×10^5 M^{-1}), which is higher than that of the typical intercalator EB (K_b =1.23(±0.07)×10^5 M^{-1}).

<<<Insert Table 3 here>>>

According to their crystal structures, **1**-**4** are metallointercalators that have reinforced binding ability to DNA because intercalative π–π stacking of the aromatic rings in the metal

complexes **1**-**4** with DNA bases can affect the transition dipoles of the molecules and lead to a reduction in their absorbance. However, because of the different nature of the metals and structures, the binding abilities of **1**-**4** to DNA are different. Although the exact mode of binding cannot be merely proposed by UV spectroscopic titration studies, the existence of hypochromism observed for **1**-**4** shows that the possibility of intercalation between the base pairs of CT DNA cannot be ruled out.

CD studies

Circular dichroism (CD) spectra of the complexes with double-stranded DNA can provide us with useful information concerning the complex-nucleotide interaction. It is generally accepted that covalent binding and intercalative binding can influence the tertiary structure of DNA and lead to changes of CD spectra for DNA, whereas other noncovalent binding modes such as electrostatic interaction or groove binding cannot significantly perturb the CD spectra.[62]

<<<Insert Figure 6 here>>>

The CD absorption of CT DNA consists of a positive band I at about 275 nm and a negative one II at 245 nm, due to the π–π base stacking of DNA and the right-hand helicity of B-form DNA, respectively.[63] The addition of HEn did not perturb the CD spectrum of DNA until HEn reached 5×10^{-5} M, when a broadening and a shift of the λ_{max} from 275 nm to lower wavelengths (down to 270 nm) is observed and the negative band II has an evident increase

(for HEn, HLevo, complexes **2**-**4**, see Fig. S5). Intercalation is the most probable binding mode between HEn and DNA due to the planar aromatic structure of HEn, but the intercalative ability appears weak. However, the addition of complex **1** induced significant changes in the characteristic absorption of DNA. As shown in Fig. 6, when **1** reached 2×10^{-5} M, band I becomes broad and is resolved to two distinct positive maxima at λ_{max} = 264 nm and λ_{max} = 277 nm, while at higher concentrations of **1** (from 3×10^{-5} M to 5×10^{-5} M) the characteristic DNA absorption peaks disappeared. The overall changes in the CD spectra of **1** indicate DNA-form changes from B- to A-form, which can be attributed to intrastrand linking of adjacent guanines so that the DNA conformation is modified and destacking of the adjacent bases occurs.[64]

For complex **2**, at DNA/**2** molar ratios from 10:0.5 to 10:4, a slight increases in the positive absorbance at λ_{max} = 275 nm were observed, while at higher concentrations of **2** (5×10^{-5} M) the characteristic DNA absorption peaks are resolved to two distinct positive maxima at λ_{max} = 267 nm and λ_{max} = 283 nm, meanwhile the maxima negative band II (λ_{max} = 246 nm) shifted to 242 nm, suggesting the transformation of DNA secondary structure.

For **3**, the gradual increase of DNA/**3** molar ratios leads to a slight decrease of the intensity and an evident bathochromism shift (from 276 nm to 282 nm) for the band I, meanwhile the negative band II shift to lower wavelengths (from 246 nm to 239 nm), indicating that **3** is bound to CT DNA. The addition of **4** did not perturb the positive band I of DNA until **4** reached 5×10^{-5} M, when a bathochromism shift (up to 280 nm) and a new peak at 267 nm is observed. While the intensity of the maxima negative band II of **4** is gradually increased.

Under the same conditions, complex **2** did not induce such dramatic changes in the CD spectrum of DNA as **1** did, which should be due to the dramatic different structure of **2** to that of **1**. The different changes in the CD spectrum of DNA for **3** and **4** may be attributed to the difference of their mononuclear structure. From all these data, we can conclude that complexes **1**-**4** all can interact with DNA and possiblely intercalative binding give a significant influence on the tertiary structure of DNA according to changes of CD spectra for DNA, but we cannot safely suggest the exact mode of binding.

Competitive studies with ethidium bromide

Ethidium bromide (EB =3,8-Diamino-5-ethyl-6-phenyl-phenanthridinium bromide) as a phenanthridine fluorescence dye is a typical indicator of intercalation. The changes observed in the fluorescence emission spectra of EB on its binding to CT-DNA are usually utilized for the interaction study between DNA and other substances such as metal complexes.[65]

HEn, HLevo and complexes **1**–**4** show no fluorescence at room temperature in solution or in the presence of CT-DNA, so the binding of them with DNA cannot be directly predicted through the emission spectra. Hence, competitive EB binding studies have been undertaken to obtain their binding abilities to CT-DNA. In the competitive binding experiments, the emission spectra of EB-DNA system at 598 nm (λ_{ex} = 332 nm) in the absence and presence of each complex **1**-**4** or HEn/HLevo ligand at diverse *r* values have been recorded. As depicted in Fig. 7A (for HEn, HLevo and **2**–**4** see Fig. S6), when increasing the concentration of **1** from **1**/EB = 1:1 to 6:1, the characteristic emission of EB was significantly decreased. The observed moderate to significant quenching of DNA-EB fluorescence (up to 16% of the initial

EB-DNA fluorescence intensity for **1**, 81% for **2**, 22% for **3** and 77% for **4**) (Fig. 7B) suggests that they displace EB from the EB-DNA complex and they can probably interact with CT DNA by the intercalative mode.[38,66]

<<<Insert Figure 7 here>>>

The Stern–Volmer plots (Fig. S7) for the complexes illustrate that the quenching of DNA-EB complex fluorescence by the compounds is in good agreement (R = 0.98) with the linear Stern-Volmer equation (Eq. S2). The K_{sv} values calculated for the complexes are listed in Table 3. The highest K_{sv} values are provided by enoxacin copper complex **1**. All the four complexes exhibited stronger quenching ability than free HEn, HLevo ligand. As can be seen, the four complexes **1**-**4** can effectively quench the EB-DNA fluorescence, which strongly suggests that they may compete with EB to bind to DNA through intercalation at the similar binding site.

Binding of the complexes to serum albumins

Serum albumins are proteins involved in the transport of metal ions and metal complexes with drugs through the blood stream. Due to its structural homology with human serum albumin (HSA), bovine serum albumin (BSA) is the most extensively studied serum albumin. When excited at 295 nm, HSA and BSA solutions show the characteristic strong fluorescence emission at 351 nm and 343 nm respectively due to their tryptophan residues.[67] Binding to these proteins may lead to loss or enhancement of the biological properties of the original

drug, or provide paths for drug transportation.

The interaction of HEn, HLevo and complexes **1**–**4** with HSA and BSA has been studied from tryptophan emission-quenching experiments. Upon addition of each complex **1**-**4** or HEn/HLevo ligand to the HSA or BSA system, changes and quenching are observed in the fluorescence emission spectra of tryptophan (Fig. S8 for HSA, Fig. S9 for BSA), probably due to change of protein conformation, subunit association, substrate binding or denaturation.[68] The enoxacin complexes exhibited a maximum emission at 335 nm, while for the levofloxacin complexes the maximum emission appeared at 460 nm, under the same experimental conditions the SA fluorescence spectra have been corrected before the experimental data processing.

Binding of the complexes to human serum albumin

Addition of HEn, HLevo or complexes **1**–**4** to HSA resulted in obvious fluorescence quenching (Fig. S8), the intensity of the fluorescence signal at 335 nm is decreased with the simultaneous appearance of an isoemissive point at ~369 nm and ~390 nm for the enoxacinato and levofloxacinato compounds, respectively. The quenching provoked by HEn, HLevo and the complexes (Fig. 8A) is significant (up to 29% of the initial fluorescence intensity for **1**, 82% for **2**, 28% for **3**, 27% for **4**, 47% for HEn and 36% for HLevo) because of possible changes in protein secondary structure leading to changes in tryptophan environment of HSA. These results clearly indicate the binding of HEn, HLevo or each complex to HSA, which quenches the intrinsic fluorescence of the single tryptophan in HSA.

<<<Insert Figure 8 here>>>

The values of the dynamic quenching constant (K_{sv}, M^{-1}) and the quenching constant (k_q, $M^{-1}s^{-1}$) for the interaction of HEn, HLevo or complexes **1-4** with SA have been derived according to Stern-Volmer quenching equation (Eq. S3). K_{sv} (M^{-1}) can be obtained by the slope of the diagram Io/I versus Q (Fig. S10), and subsequently the approximate k_q ($M^{-1}s^{-1}$) may be calculated.

The calculated values for the interaction of HEn, HLevo or complexes **1**–**4** with HSA are given in Table 4, which indicates good HSA binding propensity of the complexes. The k_q values increase in the order **2** < HEn < HLevo < **1** < **3** < **4** with complex **4** exhibiting the strongest HSA binding ability. As it can be seen, the k_q values (>10^{13} M^{-1} s^{-1}) are higher than diverse kinds of quenchers for biopolymers fluorescence (2.0×10^{10} M^{-1} s^{-1}) indicating that a static quenching mechanism is operative.[68]

<<<Insert Table 4 here>>>

The association binding constant K (M^{-1}) and the number of binding sites per albumin (n) can be obtained by the Scatchard equation ((Eq. S4) and their values are given in Table 4. It is obvious that K value of **1-4** are higher than that of HEn, HLevo ligand, suggesting that the coordination of HEn or HLevo to Cu^{2+} or Co^{2+} in the presence of phen or bipy results in enhanced affinity to HSA.

Binding of the complexes to bovine serum albumin

Addition of the free quinolones and their complexes **1-4** to the BSA leads to obvious decrease of the fluorescence signal intensity at 345 nm (Fig. S9) with the simultaneous

appearance of an isoemissive point ~390 nm for the levofloxacinato compounds. The quenching is up to 25% of the initial fluorescence intensity for **1**, 19% for **2**, 23% for **3**, 15% for **4**, 49% for HEn and 39% for HLevo (Fig. 8B) indicating that the binding of each compound to BSA quenches the intrinsic fluorescence of the single tryptophan in BSA. The Stern-Volmer equation applied for the interaction with BSA in Fig. S11 shows that the curves have good linear relationships (r = 0.98) according to Eq. S3. The calculated values of K_{sv} and k_q for HEn, HLevo or complexes **1**–**4** as given in Table 5, which indicates good BSA binding propensity of the four complexes. Complex **4** exhibits the strongest BSA binding ability among them.

<<<Insert Table 5 here>>>

From the Scatchard equation (Eq. S4), the association binding constant of each compound has been calculated (Table 5). It is obvious that K value of **1**-**4** are higher than that of HEn, HLevo ligand, suggesting that the coordination results in a increased affinity for BSA. The n value of **1**–**4** increases upon coordination.

Comparing the affinity of the compounds for HSA and BSA, it is evident that **2**, **3** and **4** show higher affinity for BSA than HSA, while **1** exhibits higher binding constant for HSA than BSA. In general, the binding constant of a compound to protein should be at an optimum range to allow binding and possible transfer and also to be released upon arrival at its target. It is noteworthy that the *K* values of all complexes **1**-**4** may be considered to be within such a range; they are high enough (Table 4-5) to allow the binding of a compound to SA and also

significantly below the association constant of the one of strongest known non-covalent bonds of avidin-ligands interaction ($K \sim 10^{15}$ M^{-1}), suggesting a possible release from the serum albumin to the target cells.[69] Therefore, the interaction of compounds with albumins may provide useful information concerning any potential application.

Conclusions

The synthesis and characterization of four complexes with the quinolone antibacterial drug enoxacin and levofloxacin in the presence of the 1,10-phenanthroline or 2,2′-bipyridine were achieved. **1** is a novel dinuclear copper complex, in which enoxacin exhibits a tridentate binding mode bound to two Cu(II) ions via the ketone oxygen, the carboxylate oxygen and the piperazine nitrogen atom, such mode and square structure were firstly observed in metal-quinolone complexes. In mononuclear complexes **2**-**4**, enoxacin and levofloxacin behave as a bidentate ligand bound to the metal through the ketone oxygen and carboxylate oxygen atom. The antimicrobial activity of the complexes **1**-**4** were tested against four bacterial species showing that they exhibit significant activity (MIC = 0.066~4.087 $\mu g \cdot mL^{-1}$) and some of them are obviously higher than the corresponding free quinolone antibacterial drugs.

UV spectroscopy and CD studies revealed the ability of the complexes to bind to CT DNA and existing of intercalation interaction to CT DNA. The binding strength of the complexes with CT DNA calculated with UV spectroscopic titrations showed that **1**-**4** exhibit higher binding constants to CT DNA than free quinolone drugs. The enoxacin cobalt complex **2** had the highest K_b values (6.04×10^5) among the complexes examined, which is higher than

the K_b value of typical indicator of intercalation EB (1.23×10^5). In the CD spectrum of DNA, under the same conditions, complex **1** induced more dramatic changes than that of **2** due to the dramatic different structure of **1** to that of **2** and the different changes for **3** and **4** mainly attributed to the difference of the mononuclear structure. Competitive binding studies with EB revealed the ability of the complexes to displace the typical intercalator EB from the EB-CT DNA complex suggesting intercalation as a possible mode of their interaction with CT DNA. All the four complexes exhibited stronger quenching ability than free HEn, HLevo ligand. The highest K_{sv} values (7.99×10^4) are provided by enoxacin copper complex **1**. Additionally, the interaction of all complexes with bovine or human serum albumins proteins were studied by fluorescence spectroscopy revealing their good binding affinity to BSA and HSA with relatively high binding constants.

In conclusion, the four new complexes present promising biological features. Further experiments in relation to other potential biological activity of the complexes such as antitumor are under consideration.

Acknowledgements

The authors thank the financial support by Jiangsu National Science Foundation (No. BK2009239). The project was also funded by Key Laboratory for the Chemistry and Molecular Engineering of Medicinal Resources (Guangxi Normal University), Ministry of Education of China (CMEMR2013-B02).

Appendix A. Supplementary material.

CCDC 995246-995249 contains the supplementary crystallographic data for this paper. These data can be obtained free of charge via http://www.ccdc.cam.ac.uk/conts/retrieving.html, or from the Cambridge Crystallographic Data Centre, 12 Union Road, Cambridge CB2 1EZ, UK; fax: (+44) 1223-336-033; or e-mail: deposit@ccdc.cam.ac.uk.

Supplementary data associated with this article can be found in the online version, at doi:

References

1 A. Tarushi, C.P. Raptopoulou, V. Psycharis, A. Terzis and G. Psomas, *Bio. Med. Chem.,* 2010, **18**, 2678-2685.

2 I. Turel, *Coord. Chem. Rev.*, 2002, **232**, 27-47.

3 L.A. Mitscher, *Chem. Rev.*, 2005, **105**, 559–592.

4 D.C. Hooper, *Biochim. Biophys. Acta.*, 1998, **1400**, 45-61.

5 L.L. Shen, W.E. Kohlbrenner, D. Weigl and J. Baranowski, *J. Biol. Chem.*, 1989, **264**, 2973-2978.

6 B. Macias, M.V. Villa, I. Rubio, A. Castineiras and J. Borras, *J. Inorg. Biochem.*, 2001, **84**, 163-170.

7 J. Robles, J. Martín-Polo, L. Álvarez-Valtierra, L. Hinojosa and G.D. Mendoza, *Met. Based Drugs*, 2000, **7**, 301–311.

8 E.K. Efthimiadou, Y. Sanakis, M. Katsarou, C.P. Raptopoulou, A. Karaliota, I. Katsaros and G. Psomas, *J. Inorg. Biochem.*, 2006, **100**, 1378–1388.

9 G. Lipunova, E. Nosova and V. Charushin, Russ. *J. Gen. Chem.*, 2009, **79**, 2753–2766.

10 M.P. Lopez-Gresa, R. Ortiz, L. Perello, J. Latorre, M. Liu-Gonzalez, S. Garcia-Granda, M. Perez-Priede and E. Canton, *J. Inorg. Biochem.*, 2002, **92**, 65–74.

11 D. Shingnapurkar, R. Butcher, Z. Afrasiabi, E. Sinn, F. Ahmed, F. Sarkar and S. Padhye, *Inorg. Chem.*

Commun., 2007, **10**, 459–462.

12 B. Macias, M.V. Villa, M. Sastre, A. Castineiras and J. Borras, *J. Pharm. Sci.*, 2002, **91**, 2416–2423.

13 R. Saraiva, S. Lopes, M. Ferreira, F. Novais, E. Pereira, M.J. Feio and P. Gameiro, *J. Inorg. Biochem.*, 2010, **104**, 843–850.

14 A. Serafin and A. Stanczak, Russ. *J. Coord. Chem.*, 2009, **35**, 81–95.

15 K.C. Skyrianou, E.K. Efthimiadou, V. Psycharis, A. Terzis, D.P. Kessissoglou and G. Psomas, *J. Inorg. Biochem.*, 2009, **103**, 1617–1625.

16 I. Sousa, V. Claro, J.L. Pereira, A.L. Amaral, L. Cunha-Silva, B. de Castro, M.J. Feio, E. Pereira and P. Gameiro, *J. Inorg. Biochem.*, 2012, **110**, 64–71.

17 S.C. Wallis, B.G. Charles, L.R. Gahan, L.J. Filippich, M.G. Bredhauer and P.A. Duckworth, *J. Pharm. Sci.*, 1996, **85**, 803–809.

18 G.G. Wu, G.P. Wang, X.C. Fu and L.G. Zhu, *Molecules*, 2003, **8**, 287–296.

19 C.Y. Chen, Q.Z. Chen, X.F. Wang, M.S. Liu and Y.F. Chen, *Transit. Met. Chem.*, 2009, **34**, 757–763.

20 D. K. Saha, U. Sandbhor, K. Shirisha, S. Padhye, D. Deobagkar, C. E. Anson and A. K. Powell, *Bioorg. Med. Chem. Lett.*, 2004, **14**, 3027-3032.

21 A. Tarushi, J. Kljun, I. Turel, A. A. Pantazaki, G. Psomas and D. P. Kessissoglou, *New. J. Chem.*, 2013, **37**, 342.

22 J. Hernandez-Gil, L. Perello, R. Ortiz, G. Alzuet, M. Gonzalez-Alvarez and M. Liu-Gonzalez, *Polyhedron*, 2009, **28**, 138–144.

23 P. Fernandes, I. Sousa, L. Cunha-silva, M. Ferreira, B.D. Castro, E.F. Pereira, M. J. Feio and P. Gameiro, *J. Inorg. Biochem.*, 2014, **131**, 21–29.

24 N.R. Cozzarelli, *Science*, 1980, **207**, 953–960.

25 J.Q. Sha, X. Li, H.B. Qiu, Y.H. Zhang and H. Yan, *Inorg. Chim. Acta.*, 2012, **383**, 178-184.

26 Z.F. Chen, L.C. Yu, D.C. Zhong, H. Liang, X.H. Zhu and Z.Y. Zhou, *Inorg. Chem. Commun.*, 2006, 9839-843.

27 Y.X. Li, Z.F. Chen, R.G. Xiong, Z.L. Xue, H.X. Ju and X.Z. You, *Inorg. Chem. Commun.*, 2003, **6**, 819-822.

28 E.K. Efthimiadou, Y. Sanakis, C.P. Raptopoulou, A. Karaliota, N. Katsaros and G. Psomas, *Bioorg. Med. Chem. Lett.*, 2006, **16**, 3864-3867.

29 Y.Ch. Liu, Zh.F. Chen, Sh.M. Shi, H.Sh. Luo, D.Ch. Zhong, H.L. Zou and H. Liang, *Inorg. Chem. Commun.*, 2007, **10**, 1269-1272.

30 L.C. Yu, Z.L. Tang, P.G. Yi and S.L. Liu, *J. Coord. Chem.*, 2009, **62**, 894-902.

31 J.C. McGregor, G.P. Allen and D.T. Bearden, *Ther. Clin. Risk. Manag.*, 2008, **4**, 843–853.

32 K. Sato, H. Tomioka, T. Akaki and S. Kawahara, *Int. J. Antimicrob. Agents*, 2000, **16**, 25–29.

33 G. Song, Y. He and Z. Cai, *J. Fluoresc.*, 2004, **14**, 705–710.

34 P. Drevensek, J. Kosmrlj, G. Giester, T. Skauge, E. Sletten, K. Sepcic and I. Turel, *J. Inorg. Biochem.* 2006, **100**, 1755–1763.

35 L. C. Yu, Z. L. Tang, P.G. Yi, S.L. Liu and X. Li, *J. Coord. Chem.*, 2008, **61**, 2961-2967.

36 P. Zivec, F. Perdih, I. Turel, G. Giester and G. Psomas, *J. Inorg. Chem.*, 2012, **117**, 35-47.

37 L.C. Yu, L. Lai, R. Xia and S.L. Liu, *J. Coord. Chem.*, 2009, **62**, 1313-1319.

38 A. Tarushi, E. Polatoglou, J. Kljun, I. Turel, G. Psomas and D.P. Kessissoglou, *Dalton. Trans.*, 2011, **40**, 9461–9473.

39 I. Turel, J. Kljun, F. Perdih, E. Morozova, V. Bakulev and N. Kasyanenko, *Inorg. Chem.*, 2010, **49**, 10750-10752.

40 J. Kljun, I. Bratsos, E. Alessio, G. Psomas, U. Repnik, M. Butinar, B. Turk and I. Turel, *Inorg. Chem.*, 2013, **52**, 9039-9052.

41 I. Sousa, V. Claro, J.L. Pereira, A.L. Amaral, L.C. Silva, B.D. Castro, M.J. Feio, E. Pereira and P. Gameiro, *J. Inorg. Biochem.*, 2012, **110**, 64-71.

42 R.R. Crichton, Biological Inorganic Chemistry: an introduction, Elsevier, Amsterdam, 2008.

43 M.E. Katsarou, E.K. Efthimiadou, G. Psomas, A. Karaliota and D. Vourloumis, *J. Med. Chem.*, 2008, **51**, 470–478.

44 G. Psomas, A. Tarushi, E.K. Efthimiadou, Y. Sanakis, C.P. Raptopoulou and N. Katsaros, *J. Inorg. Biochem.*, 2006, **100**, 1764–1773.

45 P.J. Sadler, *Adv. Inorg. Chem.*, 1991, **36**, 1–48.

46 P.V. Bernhardt, G.A. Lawrance, J.A. McCleverty and T.J. Meyer, *Comprehensive Coordination Chemistry II*. 2003, **6**, 1–45.

47 C.V. Kumar, J. K. Barton and N. J. Turro, *J. Am. Chem. Soc.*, 1985, **107**, 5518−5523

48 M. F. Reichmann, S. A. Rice, C. A. Thomas and P. Doty, *J. Am. Chem. Soc.*, 1954, **76**, 3047−3053.

49 G.M. Sheldrick, SHELXS-97, Program for Crystal Structure Solution, University of Göttingen, Germany, 1997.

50 G.M. Sheldrick, SHELXL-97, Program for Crystal Structure Refinement, University of Göttingen, Germany, 1997.

51 Y. Hua, Y. Liu, J. Wang, X. Xiao and S. Qu, *J. Pharm. Biomed. Anal.*, 2004, **36**, 915–919.

52 K. Nakamoto, Infrared and Raman Spectra of Inorganic and Coordination Compounds, Part B: Applications in Coordination, Organometallic, and Bioinorganic Chemistry, 6th ed. Wiley, New Jersey, 2009.

53 E. Chalkidou, F. Perdih, I. Turel, D.P. Kessissoglou and G. Psomas, *J. Inorg. Biochem.*, 2012, **113**, 55-65.

54 Z.F. Chen, Y.F Shi, Y.C. Liu, X. Hong, B. Geng, Y. Peng and H. Liang, *Inorg. Chem.*, 2012, **51**, 1998-2009.

55 A. W. Addison, T.N. Rao, J. Reedijk, J. van Rijn and G.C. Verchoor, *J. Chem. Soc. Dalton Trans.*, 1984, 1349–1356.

56 D. Cremer and J.A. Pople, *J. Am. Chem. Soc.*, 1975, **97**, 1354–1358.

57 E. K. Efthimiadou, M. Katsarou, Y. Sanakis, C.P. Raptopoulou, A. Karaliota, N. Katsaros and G. Psomas, *J. Inorg. Biochem.*, 2006, **100**, 1378–1388.

58 G. Psomas, C. Dendrinou-Samara, P. Philippakopoulos, V. Tangoulis, C.P. Raptopoulou, H. Samaras and D.P. Kessissoglou, *Inorg. Chim. Acta.*, 1998, **272**, 24–32.

59 A. Tarushi, C.P. Raptopoulou, V. Psycharis, A. Terzis, G. Psomas and D.P. Kessissoglou, *Bioorg. Med. Chem*. 2010, **18**, 2678–2685.

60 T.M. Kelly, A.B. Tossi, D.J. McConnell and T.C. Strekas, *Nucleic Acids Res.*, 1985, **13**, 6017–6034.

61 Y. Song, Q. Wu, P. Yang, N. Luan, L. Wang, Y. Liu, *J. Inorg. Biochem.*, 2006, **100**, 1685–1691.

62 L. Messori, P. Orioli, C. Tempi and G. Marcon, *Biochem. Biophys. Res. Commun.*, 2001, **281**, 352−360.

63 S. Schafe, I. Ott, R. Gust and W.S. Sheldrick, *Eur. J. Inorg. Chem.*, 2007, 3034−3046.

64 E.K. Efthimiadou, G. Psomas, Y. Sanakis, N. Katsaros and A. Karaliota, *J. Inorg. Biochem.*, 2007, **101**, 525−535.

65 G.H. Zhao, H.K. Lin, S.R. Zhu, H.W. Sun and Y.T. Chen, *J. Inorg. Biochem.*, 1998, **70**, 219–226.

66 K.C. Skyrianou, F. Perdih, A.N. Papadopoulos, I. Turel, D.P. Kessissoglou and G. Psomas, *J. Inorg. Biochem.*, 2011, **105**, 1273–1285.

67 J.R. Lakowicz, Principles of Fluorescence Spectroscopy, 2nd ed. Plenum Press, New York, 1999.

68 Y. Wang, H. Zhang, G. Zhang, W. Tao and S. Tang, *J. Luminescence*, 2007, **126**, 211–218.

69 V. Rajendiran, R. Karthik, M. Palaniandavar, H. Stoeckli-Evans, V.S. Periasamy, M.A. Akbarsha, B.S. Srinag and H. Krishnamurthy, *Inorg. Chem.*, 2007, **46**, 8208–8221.

Figure and table captions

Table 1 Crystallographic data and structure refinement summary for complexes **1**–**4**.

Table 2 Minimal inhibitory concentrations (MICs, $\mu g \cdot mL^{-1}$).

Table 3 The DNA binding constants (K_b) and the Stern–Volmer constants (K_{sv}) for HEn, HLevo and complexes **1**–**4**.

Table 4 The HSA binding constants and parameters derived for HEn, HLevo and complexes **1**–**4**.

Table 5 The BSA binding constants and parameters derived for HEn, HLevo and complexes **1**–**4**.

Fig. 1. The dinuclear structure of **1**. The ClO_4^-, hydrogen atoms and water molecules are omitted for clarity.

Fig. 2. Molecule structure of complex **2**. The ClO_4^-, hydrogen atoms and water molecules are omitted for clarity.

Fig. 3. Molecule structure of complex **3**. The ClO_4^-, hydrogen atoms and water molecules are omitted for clarity.

Fig. 4. Molecule structure of complex **4**. The ClO_4^-, hydrogen atoms and water molecules are omitted for clarity.

Fig. 5. UV absorption spectra of **1** (A) and **4** (B) in the absence (---) and presence (—) of CT DNA with increasing DNA / compound ratios range from 0.5:1 to 6:1. The arrows show the changes upon increasing amounts of CT DNA. Inset: plot of DNA /(ε_a-ε_f) versus DNA.

Fig. 6. Circular dichroism spectra of CT DNA bound by **1** with DNA/**1** ratios range from 10:0.5 to 10:5 (DNA alone of 1×10^{-4} M, dashed line; DNA bound by **1** with increasing concentrations, colored solid lines).

Fig. 7. (A) Fluorescence emission spectra of EB-DNA in the absence (dashed line) and presence of increasing amounts of **1** (colored solid lines) with **1**/EB ratios from 1:1 to 6:1. (B) Plot of EB relative fluorescence intensity (I/I_0%) vs r (r = complex/DNA) for complexes **1**-**4** and HEn, HLevo in TBS buffer solution.

Fig. 8. (A) Plot of relative fluorescence intensity at 351 nm (I/I_0%) vs r (r = compound/HSA for complexes **1**–**4**. (B) Plot of relative fluorescence intensity at 343 nm (I/I_0%) vs r (r = compound/BSA for complexes **1**–**4**.

Table 1 Crystallographic data and structure refinement summary for complexes **1**–**4**.

Complex	**1**	**2**	**3**	**4**
Formula	$C_{50}H_{54}N_{12}O_{17}F_2Cl_2Cu_2$	$C_{42}H_{51}N_8O_{14}F_2ClCo$	$C_{28}H_{33}N_5O_{11}FClCu$	$C_{48}H_{64}N_8O_{24}F_2Cl_2Co$
Fw.	1331.04	1024.29	733.59	1304.91
Temp. (K)	273(2)	296(2)	296(2)	296(2)
Cryst syst.	Triclinic	Triclinic	Triclinic	Monoclinic
Space group	*P*-1	*P*-1	*P*-1	*C2/c*
a (Å)	10.401(3)	13.2744(14)	10.598(3)	20.360(11)
b (Å)	14.123(4)	13.713(2)	10.710(3)	32.323(16)
c (Å)	19.125(6)	14.1741(15)	15.085(4)	10.184(5)
α (°)	90.608(8)	81.403(12)	80.410(4)	90
β (°)	96.072(9)	64.381(10)	86.353(4)	109.733(6)
γ (°)	99.224(9)	89.639(11)	69.459(3)	90
V (Å^3)	2756.4(14)	2295.5(5)	1580.9(7)	6309(6)
Z	2	2	2	4
Dc (g/cm^3)	1.601	1.479	1.541	1.357
μ (mm^{-1})	0.959	0.515	0.849	0.443
R_{int}	0.1385	0.0259	0.0254	0.0861
R_1 $I > 2\sigma(I)$	0.1015	0.0706	0.0459	0.0987
wR_2 (all data)	0.2222	0.2097	0.1579	0.3029
GOF on F^2	1.076	1.146	1.073	1.097

Table 2 Minimal inhibitory concentrations (MICs, μg·mL^{-1}).

Complex	Gram(+)		Gram(-)	
	B. subtilis	*S. aureus*	*P. aeruginosa*	*E. coli*
1	1.086	4.087	1.685	2.381
2	0.901	2.227	1.361	2.054
3	0.141	1.089	0.761	0.351
4	0.066	1.041	0.803	0.622
HEn	2.011	2.611	2.871	1.769
HLevo	0.091	0.679	0.213	0.514
bipy	>100	>100	>100	>100
phen	5.949	7.874	14.375	5.562

Table 3 The DNA binding constants (K_b) and the Stern–Volmer constants (K_{sv}) for HEn, HLevo and complexes **1**–**4**.

Compound	K_b (M^{-1})	K_{sv} (M^{-1})
1	7.41×10^4	7.99×10^4
2	6.04×10^5	3.58×10^3
3	2.36×10^4	6.12×10^4
4	3.68×10^4	4.95×10^3
HEn	2.09×10^4	1.28×10^3
HLevo	2.36×10^4	1.00×10^3

Table 4 The HSA binding constants and parameters derived for HEn, HLevo and complexes **1**–**4**.

Compound	K_{sv} (M^{-1})	k_q(M^{-1} s^{-1})	K (M^{-1})	n
1	1.21×10^5	1.21×10^{13}	5.74×10^4	1.33
2	7.30×10^3	7.30×10^{11}	2.37×10^4	0.44
3	1.76×10^5	1.76×10^{13}	3.51×10^4	1.74
4	2.34×10^5	2.34×10^{13}	6.65×10^4	1.51
HEn	3.72×10^4	3.72×10^{12}	1.69×10^4	1.58
HLevo	5.89×10^4	5.89×10^{12}	2.35×10^4	1.55

Table 5 The BSA binding constants and parameters derived for HEn, HLevo and complexes **1**–**4**.

Compound	K_{sv} (M^{-1})	k_q(M^{-1} $s^{-1)}$	K ($M^{-1)}$	n
1	1.22×10^5	1.22×10^{13}	4.97×10^4	1.32
2	1.40×10^5	1.40×10^{13}	6.43×10^4	1.29
3	1.12×10^5	1.12×10^{13}	5.66×10^4	1.29
4	1.81×10^5	1.81×10^{13}	7.36×10^4	1.35
HEn	3.50×10^4	3.50×10^{12}	4.91×10^4	0.88
HLevo	5.28×10^4	5.28×10^{12}	3.53×10^4	1.19

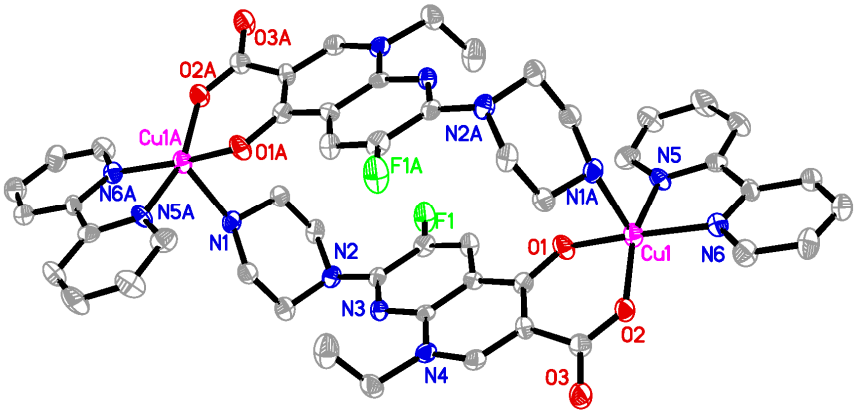

Fig. 1. The dinuclear structure of **1**. The ClO_4^-, hydrogen atoms and water molecules are omitted for clarity.

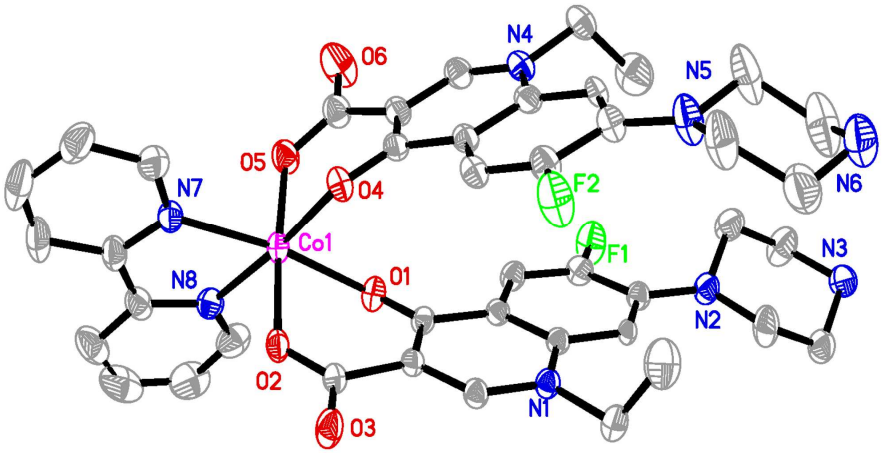

Fig. 2. Molecule structure of complex **2**. The ClO_4^-, hydrogen atoms and water molecules are omitted for clarity.

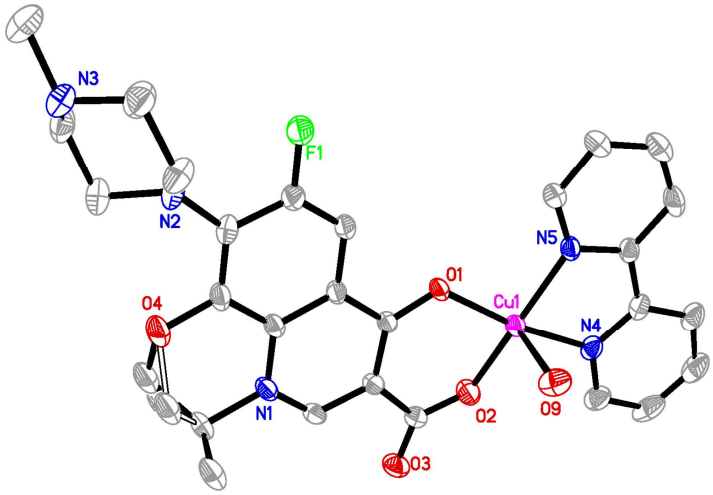

Fig. 3. Molecule structure of complex **3**. The ClO_4^-, hydrogen atoms and water molecules are omitted for clarity.

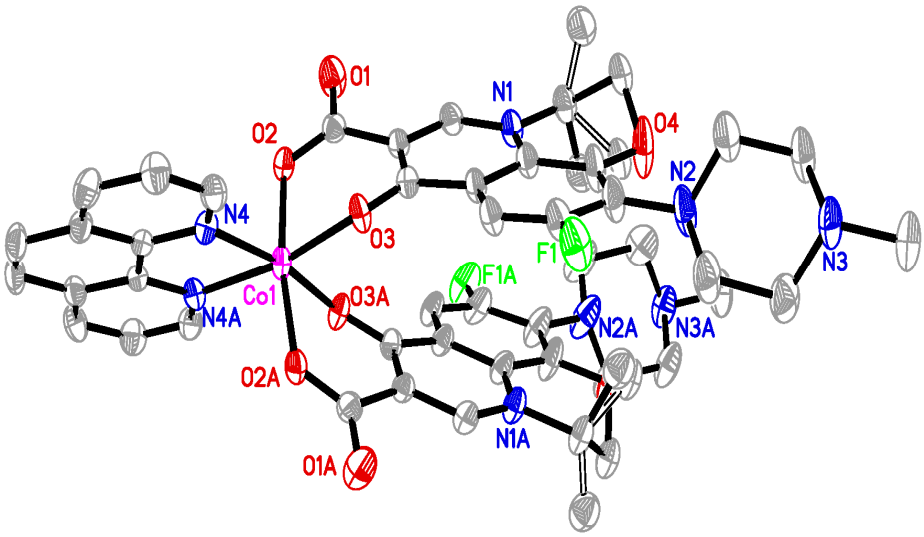

Fig. 4. Molecule structure of complex **4**. The ClO_4^-, hydrogen atoms and water molecules are omitted for clarity.

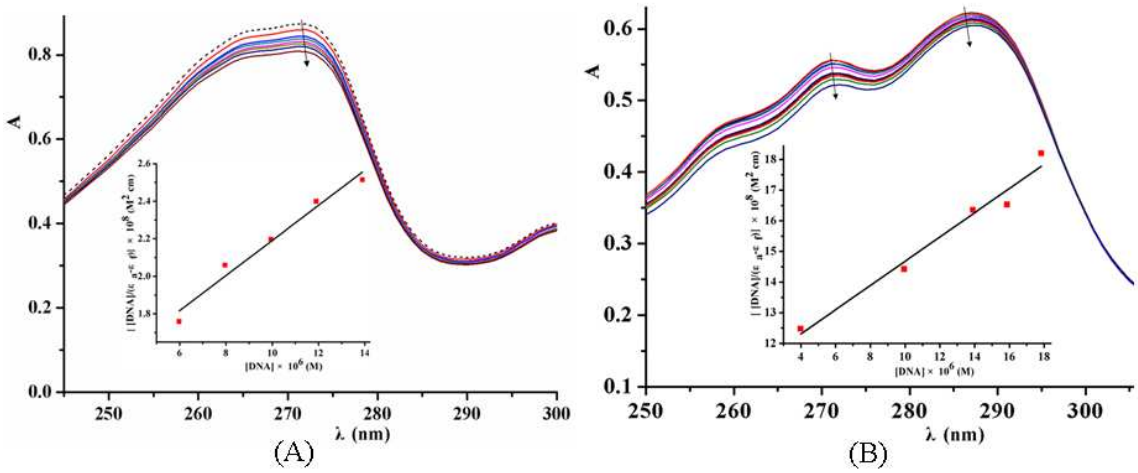

Fig. 5. UV absorption spectra of **1** (A) and **4** (B) in the absence (---) and presence (—) of CT DNA with increasing DNA/compound ratios range from 0.5:1 to 6:1. The arrows show the changes upon increasing amounts of CT DNA. Inset: plot of DNA/(ε_a-ε_f) versus DNA .

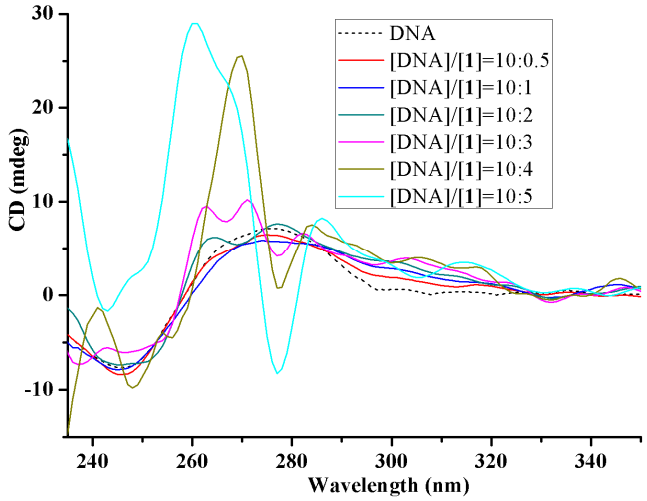

Fig. 6. Circular dichroism spectra of CT DNA bound by **1** with DNA/**1** ratios range from 10:0.5 to 10:5 (DNA alone of 1×10^{-4} M, dashed line; DNA bound by **1** with increasing concentrations, colored solid lines).

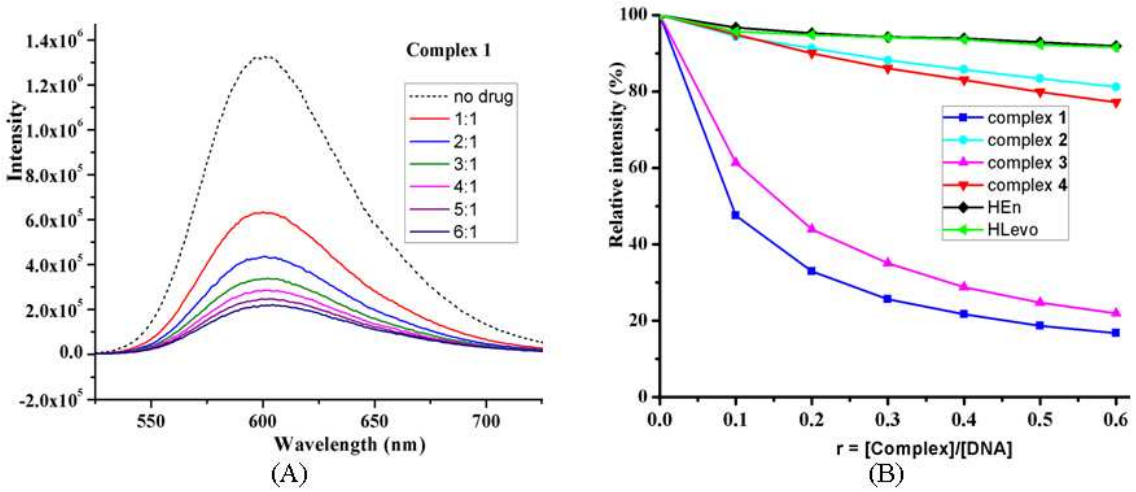

Fig. 7. (A) Fluorescence emission spectra of EB-DNA in the absence (dashed line) and presence of increasing amounts of **1** (colored solid lines) with **1**/EB ratios from 1:1 to 6:1. (B) Plot of EB relative fluorescence intensity (I/I_0%) vs r (r = complex/DNA) for complexes **1**-**4** and HEn, HLevo in TBS buffer solution.

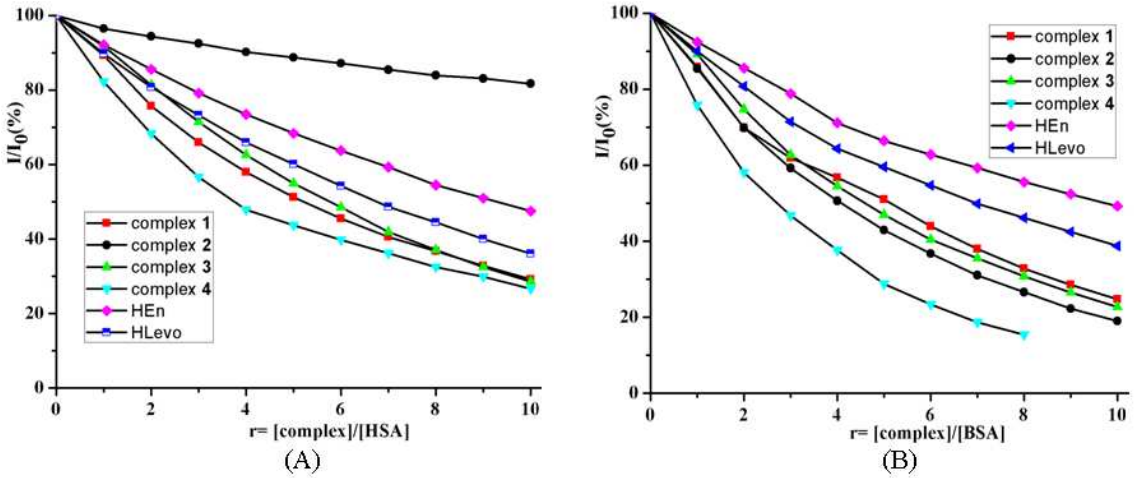

Fig. 8. (A) Plot of relative fluorescence intensity at 351 nm (I/I_0%) vs r (r = compound/HSA for complexes **1**–**4**. (B) Plot of relative fluorescence intensity at 343 nm (I/I_0%) vs r (r = compound/BSA for complexes **1**–**4**.

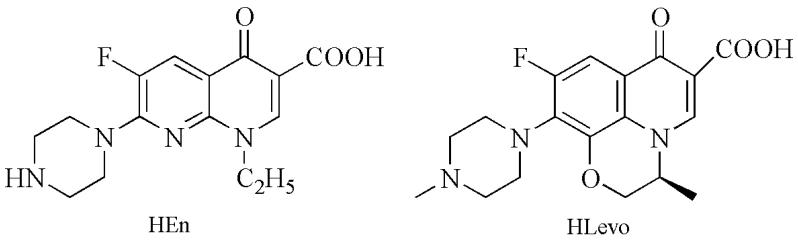

Scheme 1. (a) Enoxacin (HEn) and (b) Levofloxacin (HLevo)